Geophysical Research Letters

RESEARCH LETTER
10.1029/2019GL082094

Satellite-Based Estimation of Cloud Top Radiative Cooling Rate for Marine Stratocumulus

Youtong Zheng[1], Daniel Rosenfeld[2], Yannian Zhu[3], and Zhanqing Li[1]

[1]Earth System Science Interdisciplinary Center, University of Maryland, College Park, MD, USA, [2]Institute of Earth Sciences, The Hebrew University of Jerusalem, Jerusalem, Israel, [3]Meteorological Institute of Shaanxi Province, Xi'an, China

Key Points:
- Cloud top radiative cooling rate (CTRC) is a fundamental physical variable for understanding many essential behaviors of marine low clouds
- More accurate retrieval of CTRC is feasible from satellite with a retrieval uncertainty of 10% demonstrated by comparing them with "ground truth"
- A single summertime climatology of CTRC over the Southern Hemisphere oceans is generated, showing physically coherent results

Supporting Information:
- Supporting Information S1

Correspondence to:
Y. Zheng,
zhengyoutong@gmail.com

Citation:
Zheng, Y., Rosenfeld, D., Zhu, Y., & Li, Z. (2019). Satellite-based estimation of cloud top radiative cooling rate for marine stratocumulus. *Geophysical Research Letters*, *46*, 4485–4494. https://doi.org/10.1029/2019GL082094

Received 16 JAN 2019
Accepted 3 APR 2019
Accepted article online 5 APR 2019
Published online 17 APR 2019

Abstract Cloud top radiative cooling rate (CTRC) is the leading term in the energy budget of a marine boundary layer capped by stratocumulus. It plays a significant role in the formation, evolution, and maintenance of the stratocumulus cloud system. This study demonstrates the feasibility of estimating the CTRC, with high accuracy, from passive satellite data only. The estimation relies on a radiative transfer model with inputs from satellite-retrieved cloud parameters in combination with reanalysis sounding that is revised, in a physically coherent way, by satellite data. The satellite-based estimates CTRC agree with ground-based ones to within ~10%. The high accuracy largely benefits from the good capability of satellite data in constraining parameters of most influence to the CTRC such as free-tropospheric sounding, cloud top temperature, and cloud optical depth. Applying this technique, we generate a climatology of CTRC during summer over the Southern Hemisphere tropical and subtropical oceans.

Plain Language Summary Everything cools radiatively. For marine low-lying clouds, the radiative cooling at the cloud top makes the ambient air heavier and sink and, equivalently, the underlying air lighter and float. This forms a vertical mixing process that brings moisture from the underlying sea surfaces upward to feed the clouds, preventing them from dissipation. Therefore, the cloud top radiative cooling rate (CTRC) is one of the most important variables for understanding the behaviors of marine low clouds and their interactions with the Earth's climate system. Despite its significance, the CTRC has rarely been retrieved, with good accuracy, from satellite, the only observational tool that offers global coverage. This study fills this gap by developing a novel remote sensing method to estimate the CTRC from satellite data at an accuracy of 10%. This new capability will help advance our understanding of many poorly understood behaviors of marine low clouds over regions with scarce observations (e.g., middle- and high-latitude oceans). More broadly, the new remote sensing products will improve the accuracy with which the future climate is predicted because our climate system is sensitive to the low cloud mixing process that is regulated by the CTRC.

1. Introduction

Marine stratocumulus (Sc) is critical to the Earth's energy budget, not only because of its extensive coverage but also because of its strong negative net radiative effect (Hartmann et al., 1992; Stephens, 2005; Stephens & Greenwald, 1991). A small perturbation to Sc cloud cover and depth is sufficient to offset the warming effect of greenhouse gases (Slingo, 1990). The extensive and solid Sc decks undergo strong longwave radiative cooling that concentrates at the cloud top. Such a longwave cooling is partially offset by solar insolation during the daytime, but in most conditions it is sufficiently strong to destabilize the boundary layer and sustain the Sc. Additionally, cloud top radiative cooling (CTRC) is the dominant cooling term in the energy budget of a Sc-topped boundary layer (STBL). Changes in CTRC are typically associated with adjustment in entrainment or surface fluxes for balancing the cooling. These two functions of CTRC make it a fundamental process that regulates many aspects of the STBL system including (1) the generation of turbulent kinetic energy (TKE) and updrafts (Lilly, 1968; Nicholls, 1984; Zheng et al., 2016), (2) entrainment rate and boundary layer depth (Bretherton et al., 2007; Bretherton & Wyant, 1997; Caldwell et al., 2005; Deardorff, 1976), (3) cloud microphysics (Austin et al., 1995), (4) surface latent heat fluxes and cloud-base height (Kazil et al., 2017; Zhang et al., 2005; Zheng et al., 2018), (5) the stratification (or decoupling) of STBL (Nicholls, 1984; Zheng et al., 2018), (6) emergence of multiple equilibria of STBL (Bretherton, Uchida, et al., 2010), and (7) cell broadening of mesoscale convective circulation (Zhou & Bretherton, 2019).

Among them, the CTRC effect on the TKE is perhaps the most fundamental one because it is through modulating the TKE that the CTRC regulates the other physical processes listed above. For example, increase in CTRC causes more intense updrafts to ventilate the boundary layer (Deardorff, 1976; Stevens, 2002, 2006), regulating the mass, enthalpy, and moisture budgets of the STBL. Moreover, radiatively driven updrafts, via governing the supersaturation at cloud bases, determine how many cloud condensation nuclei particles could be nucleated into cloud droplets. The updrafts could be parameterized by CTRC (Zheng et al., 2016). In this regard, the CTRC is an important variable for disentangling the impacts of meteorology (e.g., updrafts) from the aerosol cloud-mediated effects, which has long been a central challenge in aerosol-cloud-climate interactions research (Li et al., 2017; Rosenfeld, 2014; Rosenfeld et al., 2014; Rosenfeld et al., 2016; Stevens & Feingold, 2009; Tao et al., 2012).

Conventional approaches for obtaining the CTRC include direct measurements of net radiative fluxes from aircrafts (Bretherton, Wood, et al., 2010; Nicholls, 1984) or tethered balloon (Slingo et al., 1982), and, most often, indirect calculations with a radiative transfer model that ingests field campaign observations (Ghate et al., 2014; Ghate et al., 2015; Nicholls & Leighton, 1986; Wood, 2005; Zheng et al., 2016). While the former approach is expensive, the latter is more feasible and commonly used. Strictly speaking, one can only obtain the true CTRC from direct radiative fluxes measurements. A good agreement of radiative fluxes between these two methods (e.g.Nicholls, 1984 ; Slingo et al., 1982) suggests that the radiosonde-based estimations of CTRC may be regarded as the proxy of "ground truth" when there are no aircraft observations of radiative fluxes above cloud tops.

How well satellite data, in particular passive ones, constrain the CTRC estimation remains underexplored. Active satellite sensors have been used to estimate the radiative fluxes in cloudy atmosphere (Henderson et al., 2013; L'Ecuyer et al., 2008), but the vertical resolution is too coarse to resolve the CTRC that takes place chiefly near the upper several tens of meters in shallow Sc decks, not to mention the narrow swath of the active sensors and limited validations of the products. In this study, we find that by revising the reanalysis sounding in a physically coherent way, passive satellite data could offer rather accurate estimations of CTRC (~10% error). In contrast to the narrow swath of active sensors (~1 km), the much-wider coverage of passive sensors makes it uniquely important for studying the Sc.

The data and case selections are introduced in the next section. Section 3 illustrates the procedure of revising the reanalysis soundings. The robustness of the method is demonstrated by sensitivity tests and validations against radiosonde-based CTRC estimates. In section 4, the first satellite-retrieved CTRC climatology is presented for summertime marine shallow clouds over the Southern Hemisphere (SH) oceans. The discussions and conclusion will be given in section 5.

2. Data and Methodology

2.1. Ship-Based Observations

The study region is the northeast Pacific Ocean where an Atmospheric Radiation Measurement (ARM) field campaign, Marine ARM GPCI (Global Energy and Water Cycle Experiment-Cloud System Study-Pacific Cross-section Intercomparison (MAGIC), was conducted from 2012 to 2013. A cargo ship that carried the second ARM model facility sailed between the Los Angeles, California (33.7°N, 118.2°W), and Honolulu, Hawaii (21.3°N, 157.8°W). A 7 months' worth of ship-based measurements (November to December 2012; May to September 2013) are available for analysis, during which period most of the instruments were fully operational. Cloud-base heights are measured by a Vaisala Ceilometer. Radiosondes were launched four times per day. We determine the height of the inversion-layer base (z_i) by finding the altitude where the temperature minimizes below the altitude with the strongest temperature inversion. Starting from the z_i, the inversion top height was determined as the altitude where the temperature starts to decrease with altitude. The difference between the inversion-base and top height gives the inversion depth. In this study, we use the z_i to approximate the cloud top height (H_t). The reason we do not use the radar-derived H_t is that for many Sc decks capped by very sharp inversion, a small error in radar-determined H_t can cause marked changes in the moisture at the cloud top, to which the CTRC is sensitive. This approximation is safe as indicated by the excellent agreement between the H_t derived from the Ka-band ARM Zenith Radar and z_i for all the cases surveyed in this study (Figure S1 in the supporting information).

2.2. Satellite and Reanalysis Data

We use cloud retrievals from both the 15th Geostationary Operational Environmental Satellite (GOES-15) and the Moderate Resolution Imaging Spectroradiometer (MODIS) onboard the Terra satellite (MOD06). The GOES-15 data are used for comparison with the ship-borne cloud observations. As a geostationary satellite, GOES-15 allows for much more collocations with the ship observations than the Terra. GOES-15 data are obtained from the National Aeronautics and Space Administration Langley Research Center (LaRC) cloud products. The data are sampled at 4 × 4 km horizontal resolution every 30 min. Cloud quantities used in this study are cloud top temperature (T_t), cloud visible optical depth (τ), and cloud droplet effective radius (r_e), which are retrieved by visible infrared solar infrared split-window technique from the multispectral GOES imager data. Its radiance measurements in midinfrared (3.9 μm), visible (0.65 μm), and the split-window channel (10.8 μm) are primarily sensitive to changes in r_e, τ and, T_t, respectively. These cloud parameters are inferred by matching the observed radiances to model computed top-of-atmosphere radiances in precalculated lookup tables following an iterative process (Minnis et al., 1995; Minnis et al., 1998). LWP is estimated as LWP = $(2/3)\cdot r_e\cdot\tau$. T_t is used to estimate the cloud top height (H_t) using a parameterized lapse rate (Equation (8) in Wood and Bretherton, 2004). The cloud-base height (H_b) is equal to H_t minus cloud geometrical thickness that is derived from LWP assuming adiabatic clouds. During nighttime when the retrievals from visible and near infrared channels are not available, the climatological mean values of τ (10) and r_e (12 μm) are used instead. Validations of the retrieved H_t and H_b against ship-based surface measurements show overall good agreements (Figures S2a and S2b) despite an overestimated H_t is noted.

Both the European Centre for Medium-Range Weather Forecasts Interim and National Centers for Environmental Prediction/National Center for Atmospheric Research reanalysis data are used. The variables include sea surface temperature (SST), 2-m specific humidity (q_{sfc}), and the vertical profiles of temperature and specific humidity. The reanalysis data are interpolated into the ship locations to match the satellite and ship observations.

2.3. Collocation Strategy and Case Selection

The GOES-15 data were collocated with the ship tracks by sampling pixels within a 1° × 1° rectangle centering on the ship locations. In each scene, we select 3-hr ship measurements that covered a distance of ~90 km (ship speed is ~30 km/hr), comparable to the grid size of a 1° × 1° satellite scene. Only scenes with warm cloud cover greater than 90% are selected. To allow for comparison with ship-borne radiosonde measurements, each scene is selected at radiosonde launch times that are launched every 6 hr. Six hours also allow the ship to travel sufficiently long distance to avoid overlap sampling between two consecutive scenes. A total of 100 cases were selected.

3. Estimation of CTRC Using Satellite and Reanalysis Data

3.1. Case Study

Figures 1c and 1d show the vertical profiles of radiative fluxes and heating rate, respectively, for a typical daytime STBL case on 21 July 2013 during the MAGIC field campaign. The profiles are calculated by the Santa Barbara DISORT (DIScrete Ordinates Radiative Transfer) Atmospheric Radiative Transfer model (see Text S1 for detail). The inputs are from shipborne measurements except the τ and r_e. Several salient features consistent with the conventional knowledge (Ghate et al., 2015; Roach & Slingo, 1979; Stephens, 1978; Taylor et al., 1996) are noted. First, the net radiative fluxes vary little across the subcloud layer, leading to negligible radiative cooling compared with that near the cloud top. Second, the net longwave radiative fluxes decrease rapidly toward the cloud base, resulting in a radiative flux convergence and a warming effect. Third, the longwave radiative cooling at the upper several tens of meters is partially compensated by solar heating that also maximizes near the cloud top and decreases to near zero toward cloud base.

As a comparison, we use the GOES cloud retrievals of H_t, H_b, τ, and r_e and European Centre for Medium-Range Weather Forecasts reanalysis to perform the same calculations. Due to insufficient vertical resolution, the reanalysis sounding cannot resolve the temperature inversion and moisture contrast at the cloud top. To overcome this issue, we use the GOES-derived H_t and T_t to revise the reanalysis sounding. The revision involves three steps. First, we interpolate the coarse-resolution reanalysis sounding to specified vertical

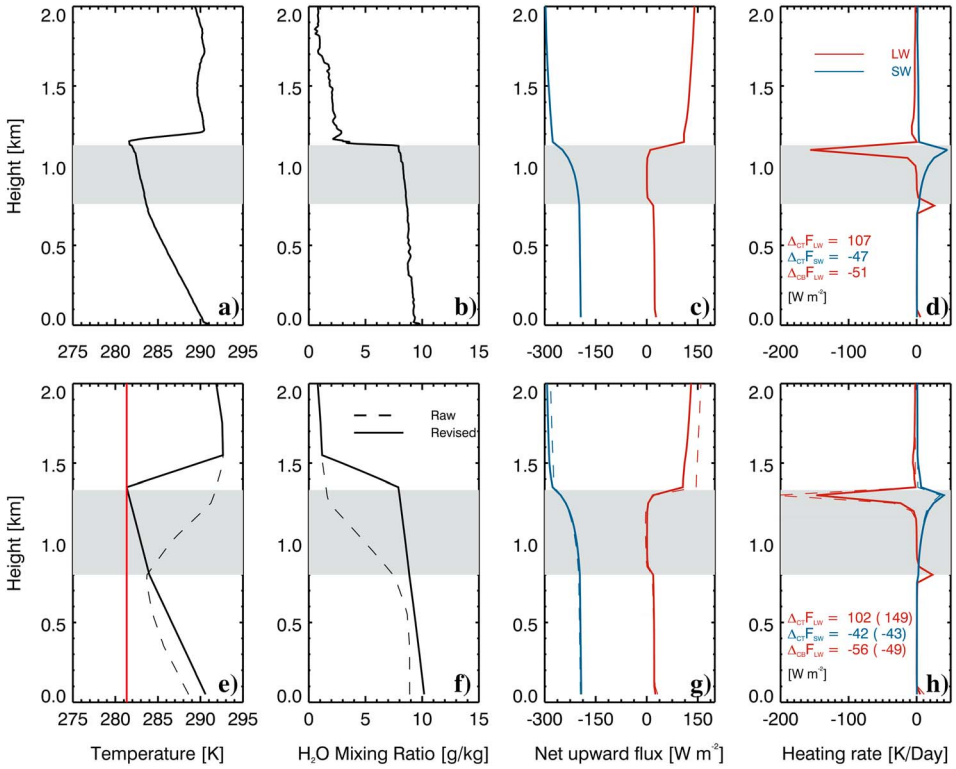

Figure 1. Profiles of temperature (a and e), water vapor mixing ratio (b and f), broadband net upward radiative fluxes (c and g), and heating rate (d and h) from radiosonde (upper panels) and reanalysis (bottom panels) for the example case. The shaded region marks the cloud boundaries. In (e), the vertical red line marks the satellite-retrieved cloud top temperature. In the bottom panels, the solid and dashed lines represent the revised and raw reanalysis, respectively.

grids with resolutions of 50 m from the surface to 2.25 km, 200 m from 2.25 to 8 km, and 3 km from 8 km above. Second, we assume a relative humidity of 100% at the cloud top and compute the cloud top water vapor density with the retrieved T_t. The in-cloud temperature and moisture soundings are adjusted by assuming a moist adiabatic cloud layer. The cloud-base values, in combination with the reanalysis data of surface temperature and water vapor mixing ratio, were interpolated to obtain the subcloud layer soundings. Finally, we specify an inversion-layer depth of 200 m. The value is based on the composite mean of inversion depth from MAGIC radiosonde measurements (187.5 ± 122.2 m). Within the inversion layer, the temperature and water vapor mixing ratio are changed linearly. There is little sensitivity to the depth of the inversion layer (see Figure S3).

Figures 1e and 1f show how the original reanalysis soundings (dashed lines) are compared with the revised ones (solid lines). A marked improvement is noted relative to the radiosonde sounding. Most importantly, the revised sounding offers a more realistic value of cloud top water vapor mixing ratio and therefore a more realistic emissivity gradient at the cloud top, to which the modeled cloud top longwave radiative cooling is sensitive. The original sounding shows too dry air overlying the cloud top, overestimating the net radiative flux divergence (Figure 1g) and the longwave cooling rate (Figure 1h) at the cloud top. To quantify this effect, we use the net radiative flux divergence between the 100 m above the cloud top and the level where the longwave radiative warming start to emerge (denoted as z^*), which is denoted as $\Delta_{CT}F$. The z^* typically locates near middle of the cloud layer depending on the cloud optical thickness. The $\Delta_{CT}F$ has both longwave ($\Delta_{CT}F_{LW}$) and shortwave ($\Delta_{CT}F_{SW}$) components. The cloud-base radiative warming is quantified as the net longwave radiative flux divergence between the z^* and 100 m below the cloud base, denoted as $\Delta_{CB}F_{LW}$. The revision has little effect on the $\Delta_{CT}F_{SW}$ and $\Delta_{CB}F_{LW}$ but considerably influences the dominant term, $\Delta_{CT}F_{LW}$. The original reanalysis sounding gives a $\Delta_{CT}F_{LW} = 149$ W/m^2, which is severely biased due to too dry overlying air (Mapes & Zuidema, 1996; Siems et al., 1993; Stevens et al., 2017; Wood, 2012). The revised $\Delta_{CT}F_{LW}$ of 102 W/m^2 is closer to the radiosonde-based value of 107 W/m^2.

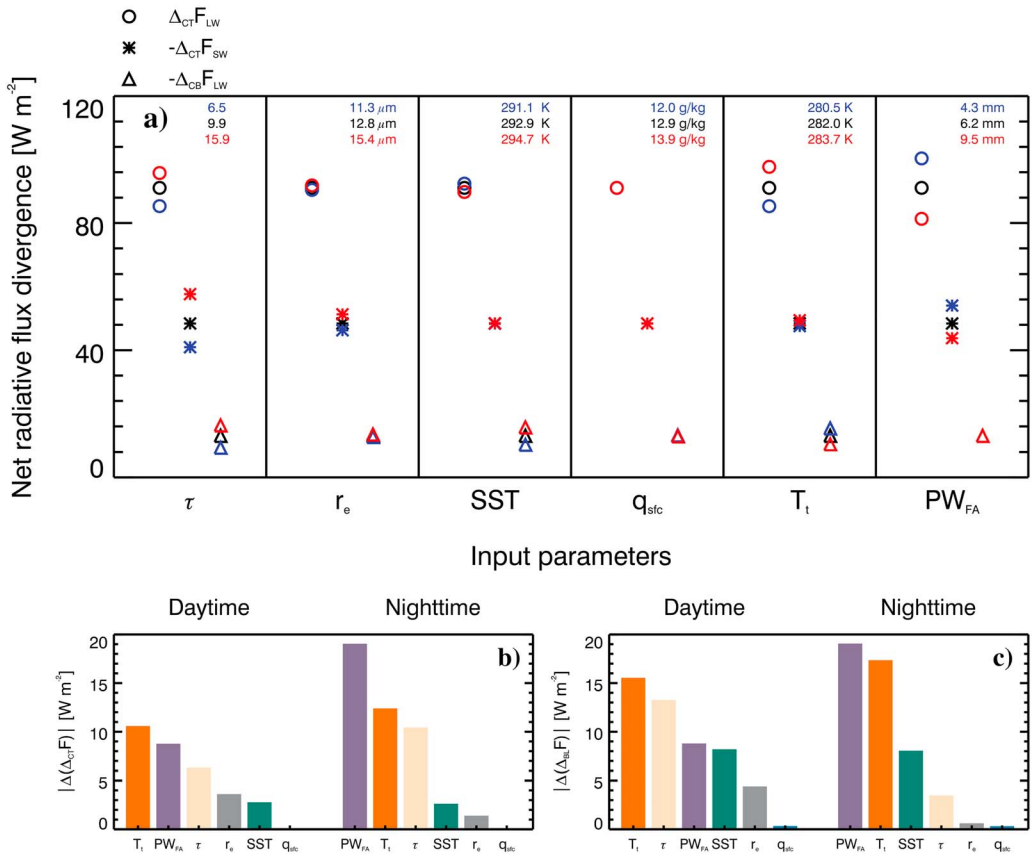

Figure 2. (a) Sensitivity of the Santa Barbara DISORT Atmospheric Radiative Transfer-calculated $\Delta_{CT}F_{LW}$ (open circle), $-\Delta_{CT}F_{SW}$ (asterisk), and $-\Delta_{CB}F_{LW}$ (open upward triangle) to the satellite/reanalysis parameters. Red, black, and blue correspond to the calculations for 25th, 50th, and 75th percentiles of the input parameters, respectively. The bottom panels show the ranking of the sensitivity of $\Delta_{CT}F$ (b) and $\Delta_{BL}F$ (c) to different input parameters. The degree of sensitivity decreases from left to the right.

3.2. Sensitivity Test

The close agreement between the satellite- and radiosonde-based CTRC motivates us to explore how sensitive the CTRC is to the different input parameters. To that end, we build up a representative case based on the composite mean of the 100 cases. The time of the case is set at 17:30 UTC on 8 July 2013 with the solar zenith angle of ~40°. Here we concentrate on two physically important CTRC-related variables: (1) $\Delta_{CT}F$ and (2) the net radiative fluxes across the entire boundary layer, $\Delta_{BL}F$, that is equal to $\Delta_{CT}F + \Delta_{CB}F_{LW}$. The Δ_{CT}F is associated with the TKE generation while the $\Delta_{BL}F$ represents the radiative energy loss that is important for the enthalpy budget of a STBL (Stevens, 2006).

We conduct a set of simple sensitivity tests by perturbing the input satellite or reanalysis parameters: (1) τ, (2) r_e, (3) SST, (4) q_{sfc}, (5) T_t, and (6) precipitable water amount above inversion-layer top (PW_{FA}). For each setting, the values of 25th (blue), 50th (black), and 75th (red) percentiles of the composite of the input parameter are employed while maintaining the other inputs unchanged (Figure 2a). We quantify the impact of each input by calculating the $|\Delta V| = |V(a^+) - V(a^-)|$, where the V could be the $\Delta_{CT}F$ or the $\Delta_{BL}F$ and a is the input parameter with the superscripts of plus and minus signs representing the 75th and 25th percentiles, respectively. In practice, perturbing the SST or T_t also causes a change in H_t, which influences the PW_{FA} (humidity decreases with altitude). To simplify the interpretation of the sensitivity results, we fix the H_t. The effect of H_t on CTRC is illustrated in the supporting information (Text S2).

Figure 2a shows that the $\Delta_{CT}F_{LW}$ (open circles) is most sensitive to PW_{FA}, T_t, and τ, and insensitive to other input parameters. The strong sensitivity to PW_{FA} is expected (Mapes & Zuidema, 1996; Siems et al., 1993; Stevens et al., 2017; Wood, 2012). Increases in T_t and τ enhance the outgoing LW radiation by increasing

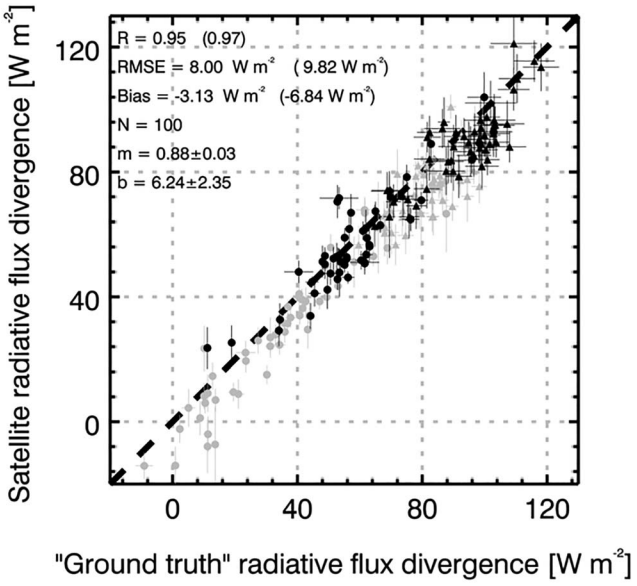

Figure 3. Comparisons between Geostationary Operational Environmental Satellite-derived $\Delta_{CT}F$ and $\Delta_{BL}F$ against Atmospheric Radiation Measurement "ground truth" cloud top radiative cooling rate. The black and gray dots represent the $\Delta_{CT}F$ and $\Delta_{BL}F$, respectively. The dots and upward triangles correspond to the daytime and nighttime cases, respectively. The correlation coefficient (R), root mean square error (RMSE), and number of cases (N) are given. The values in the parentheses correspond to the $\Delta_{BL}F$. The error bar for each point is estimated the same way as the overall error of all the samples is estimated (Text S3), but for a single case.

the emission temperature and emissivity, respectively. These three parameters dominate the sensitivity at nighttime when there is no solar heating (right in Figure 2b). When the solar heating is considered, the sensitivity decreases markedly for all the three inputs (left in Figure 2b). This is because of the cancellations, by varying degrees, between the longwave and shortwave components. For example, optically thicker clouds absorb more incoming solar radiation, compensating for the longwave radiative cooling. The degree of the cancellations largely depends on the solar zenith angle that controls the strength of solar heating (Figure S5).

The $|\Delta(\Delta_{BL}F)|$ result is overall similar to the $|\Delta(\Delta_{CT}F)|$ in terms of the strong sensitivity of the radiative heating rates to the PW_{FA}, T_t, and τ. A noticeable difference is that the SST plays a more important role in the $|\Delta(\Delta_{BL}F)|$. Increase in SST enhances the temperature gradient between the cloud-base and the surface, thus markedly enhancing the cloud-base radiative warming.

The key message conveyed by the Figure 2 is that the PW_{FA}, T_t, and τ are the three most influential factors for the radiative heating rates in a STBL. Fortunately, all of these parameters are well constrained by satellite data. The T_t and τ have long been retrieved, with good accuracy, from satellite (King et al., 1997; Minnis et al., 1992). In terms of the PW_{FA}, satellite-retrieved sounding has been considered reliable for above-cloud free troposphere (McNally et al., 2006; Susskind et al., 1998; Susskind et al., 2003) where the weighting function of a satellite-borne infrared sounder typically maximizes (Chazette et al., 2014). Although the reanalysis soundings assimilate not only the satellite but also the radiosonde data, we still expect the reanalysis sounding to work well in radiosonde-free regions because of the inherent merit of satellite infrared sounder in retrieving the PW_{FA} as discussed above. Comparison between the reanalysis- and radiosonde-derived PW_{FA} for all the selected cases shows a good agreement (Figure S1c). The PW_{FA} and the T_t are available from satellite in both nighttime and daytime. Given that the τ plays a comparatively weaker role than the PW_{FA} and T_t at night (Figure 2b and, in particular, Figure 2c), retrieval of nighttime cooling rate is principally feasible.

3.3. Systematic Validation

Figure 3 shows the validations of the satellite-retrieved $\Delta_{CT}F$ (black) and $\Delta_{BL}F$ (gray) against the "ground truth" for all the selected cases. The agreements are very encouraging. The relative errors for both quantities are ~10%. A slight underestimation is noted, which is primarily due to the overestimated PW_{FA} that weakens the CTRC. Using a different set of reanalysis data, National Centers for Environmental Prediction/National Center for Atmospheric Research reanalysis, yields a very similar result (Figure S6). A systematic error propagation analysis is shown in the supporting information (Text S3). The biggest source of error is from the τ at nighttime when the climatological mean value of τ is used. Given the dependence of CTRC on τ is highly nonlinear (Zheng et al., 2016), the estimation of nighttime CTRC may be much less reliable for semitransparent clouds for which the CTRC is particularly sensitive to τ. In addition, the T_t causes smaller error than the PW_{FA} not only because the T_t is better constrained by the satellite data but also because of the cancellation effect through the H_t (see discussion in Text S2).

4. A Summertime Climatology of CTRC Over the SH Oceans

A 4-monthlong climatology of $\Delta_{CT}F$ was generated from the Terra MODIS data over oceans between the 0° and 40° S during the southern summer (Figure 4). The samples are from our recent study (Rosenfeld et al., 2019) in which liquid phase clouds in 1° × 1° scenes without being obscured by high clouds are selected. The MODIS cloud retrieval algorithms are principally similar to the GOES LaRC algorithms although the LaRC uses less channels. Figure 4 shows that the spatial distribution of Δ_{CT}F anchors the occurrence frequency of

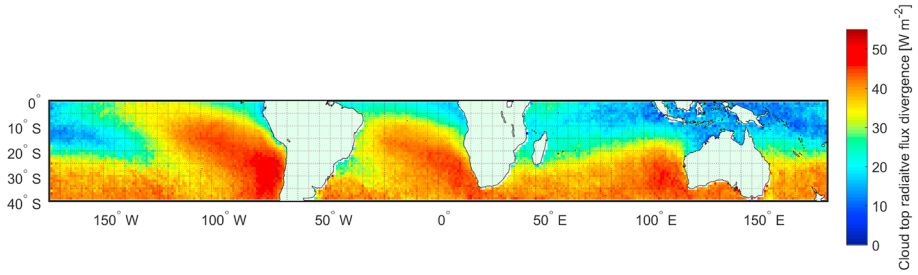

Figure 4. A summertime climatology of the $\Delta_{CT}F$ retrieved by Terra Moderate Resolution Imaging Spectroradiometer over the oceans between 0° and 40°S from November 2014 to February 2015.

Sc decks as shown in Hahn and Warren (2007). The well-known semipermanent subtropical marine Sc sheets over the subtropical eastern oceans are noticeable with the greatest $\Delta_{CT}F$. The $\Delta_{CT}F$ is markedly lower in tropical regions where the deep convection highly moistens the free atmosphere, significantly weakening the $\Delta_{CT}F$ of the underlying boundary layer clouds although the lower solar zenith angle also contributes. The similarity between the $\Delta_{CT}F$ and the occurrence frequency of Sc clouds points to the "radiatively driven" nature of the Sc. In addition, the $\Delta_{CT}F$ varies rather little (< 10 W/m^2) over the climatologically important Sc-to-cumulus transition regions, namely, the southeast Pacific (5°–30°S, 105°–70°W) and Atlantic (5°–30°S, 15°W–15°E). It is well known that there is a systematic offshore decoupling of Sc decks within these regions (Wood & Bretherton, 2004). A widely accepted theoretical explanation for the offshore decoupling is the deepening-warming theory (Bretherton & Wyant, 1997) that posits that the coastal Sc decks being advected over warmer seawater causes deeper STBLs and, via entrainment feedback, the boundary layer decoupling. An important assumption underlying this theory is the climatologically invariance of the CTRC along the tracks of Sc decks. This is well supported by our data.

Aircraft-measured radiative flux divergence during the VAMOS (Variability of the American Monsoon Systems) Ocean-Cloud-Atmosphere-Land Study Regional Experiment (VOCALS-REx) shows a marked increase in $\Delta_{CT}F_{LW}$ of ~30 W/m^2 from the Chilean coast (70°W) to 85°W along the 20°S in October–November 2008 (Bretherton, Wood, et al., 2010). Our summertime climatology shows an increase of 22 W/m^2, which is smaller than the VOCALS-REx result. Because the VOCALS-REx measurements are thought to overestimate the climatological mean $\Delta_{CT}F_{LW}$ at 85°W due to a sampling bias (Bretherton, Wood, et al., 2010), our estimate is reasonable.

5. Discussion and Conclusions

We developed a method of estimating the CTRC for marine Sc from satellite data together with corrected reanalysis data. The CTRC is calculated by a radiative transfer model with inputs from satellite-retrieved cloud quantities and satellite-corrected reanalysis sounding. A key process in the calculation is the revision of a reanalysis sounding that does not have sufficient vertical resolution to resolve the inversion layer to which the CTRC is sensitive. We use the satellite-retrieved cloud top temperature to constrain the reanalysis temperature and moisture profile by assuming a 100% relative humidity in the cloud layer and an adiabatic cloud.

The concept of revising the reanalysis sounding is not new in itself (Kablick et al., 2018; Sun-Mack et al., 2014). The originality of this study lies in applying the correction to derive the CTRC from passive satellite data at an unprecedented accuracy (~10%) even relative to that from active sensors. The retrieval uncertainty is assessed by a systematic validation against radiosonde-based CTRC estimates over the northeast Pacific. In addition, a summertime CTRC climatology over the SH tropical and subtropical oceans is generated, which shows physically reasonable distributions coherent with previous knowledge. Neither the systematic evaluation against ship measurements nor the CTRC climatology, to our knowledge, has been done before.

By conducting a set of sensitivity tests, we demonstrate why satellite data are suitable for estimating the CTRC. In a nutshell, parameters most influential to the CTRC (upper-air sounding, cloud top temperature, and cloud optical depth) can be retrieved from satellite data with good accuracy although the reanalysis data and their corrections also play an important role.

The CTRC is fundamental to many aspects of STBL dynamics. Given the large spatial and temporal coverages of satellite data, the new capability of CTRC retrieval can offer useful insights to many physical problems that are previously investigated only by local field experiments and idealized models. For example, the CTRC modulates the entrainment rate via its controls on the TKE. Too weak CTRC cannot sustain adequate entrainment to maintain the STBL against subsidence, causing the collapse of the STBL. This mechanism is the origin of the multiple equilibria of STBL that has been hypothesized analytically and found in LES large-eddy simulations (Bretherton, Wood, et al., 2010). Unambiguous observational evidence of such a mechanism is still missing. A large-scale survey of CTRC may help enlighten this problem.

All the cloud scenes studied in this work are single-layer clouds without being overlain by higher cloud layers. These elevated layer clouds can influence the CTRC by enhancing the downwelling infrared radiation reaching the Sc deck top (Christensen et al., 2013). This issue could be moderated by applying our remote sensing method (Chang & Li, 2005) that can not only detect such overlapped clouds but also derive the optical thickness and emissivity of the overlain cirrus clouds using MODIS data only. These pieces of information can be ingested into the radiative transfer model to quantify the CTRC. We plan to pursue this in the future.

Acknowledgments
Y. Z. and Z. L. are supported by the NOAA's JPSS program (NA15NWS4680011), the Department of Energy (DOE) Atmospheric System Research program (DE-SC0018996), and the National Science Foundation (AGS1837811). D. R. and Y. Z. are supported by the Joint NSFC-ISF Research Program (41561144004) and National Natural Science Foundation of China (41575136), respectively. The ground-based data in this study are available from website of ARM Climate Research Facility (www.archive.arm.gov/data). The GOES-15 cloud parameters data are obtained from the NASA Langley Cloud and Radiation Research Group (https://satcorps.larc.nasa.gov). The MODIS data are from the National Aeronautics and Space Administration (https://search.earthdata.nasa.gov). We thank two anonymous reviewers for their constructive comments.

References

Austin, P. H., Siems, S., & Wang, Y. (1995). Constraints on droplet growth in radiatively cooled stratocumulus clouds. *Journal of Geophysical Research*, *100*(D7), 14,231–14,242. https://doi.org/10.1029/95JD01268

Bretherton, C. S., Blossey, P. N., & Uchida, J. (2007). Cloud droplet sedimentation, entrainment efficiency, and subtropical stratocumulus albedo. *Geophysical Research Letters*, *34*, L03813. https://doi.org/10.1029/2006GL027648

Bretherton, C. S., Uchida, J., & Blossey, P. N. (2010). Slow manifolds and multiple equilibria in stratocumulus-capped boundary layers. *Journal of Advances in Modeling Earth Systems*, *2*, 14. https://doi.org/10.3894/JAMES.2010.2.14

Bretherton, C. S., Wood, R., George, R., Leon, D., Allen, G., & Zheng, X. (2010). Southeast Pacific stratocumulus clouds, precipitation and boundary layer structure sampled along 20 S during VOCALS-REx. *Atmospheric Chemistry and Physics*, *10*(21), 10,639–10,654. https://doi.org/10.5194/acp-10-10639-2010

Bretherton, C. S., & Wyant, M. C. (1997). Moisture transport, lower-tropospheric stability, and decoupling of cloud-topped boundary layers. *Journal of the Atmospheric Sciences*, *54*(1), 148–167. https://doi.org/10.1175/1520-0469(1997)054<0148:MTLTSA>2.0.CO;2

Caldwell, P., Bretherton, C. S., & Wood, R. (2005). Mixed-layer budget analysis of the diurnal cycle of entrainment in southeast Pacific stratocumulus. *Journal of the Atmospheric Sciences*, *62*(10), 3775–3791. https://doi.org/10.1175/JAS3561.1

Chang, F. L., & Li, Z. (2005). A new method for detection of cirrus overlapping water clouds and determination of their optical properties. *Journal of the Atmospheric Sciences*, *62*(11), 3993–4009. https://doi.org/10.1175/JAS3578.1

Chazette, P., Marnas, F., Totems, J., & Shang, X. (2014). Comparison of IASI water vapor retrieval with H_2O-Raman lidar in the framework of the Mediterranean HyMeX and ChArMEx programs. *Atmospheric Chemistry and Physics*, *14*(18), 9583–9596. https://doi.org/10.5194/acp-14-9583-2014

Christensen, M. W., Carrió, G. G., Stephens, G. L., & Cotton, W. R. (2013). Radiative impacts of free-tropospheric clouds on the properties of marine stratocumulus. *Journal of the Atmospheric Sciences*, *70*(10), 3102–3118. https://doi.org/10.1175/JAS-D-12-0287.1

Deardorff, J. (1976). On the entrainment rate of a stratocumulus-topped mixed layer. *Quarterly Journal of the Royal Meteorological Society*, *102*(433), 563–582. https://doi.org/10.1002/qj.49710243306

Ghate, V. P., Albrecht, B. A., Miller, M. A., Brewer, A., & Fairall, C. W. (2014). Turbulence and radiation in stratocumulus-topped marine boundary layers: A case study from VOCALS-REx. *Journal of Applied Meteorology and Climatology*, *53*(1), 117–135. https://doi.org/10.1175/JAMC-D-12-0225.1

Ghate, V. P., Miller, M. A., Albrecht, B. A., & Fairall, C. W. (2015). Thermodynamic and radiative structure of stratocumulus-topped boundary layers. *Journal of the Atmospheric Sciences*, *72*(1), 430–451. https://doi.org/10.1175/JAS-D-13-0313.1

Hahn, C. J., & Warren, S. G. (2007). *A gridded climatology of clouds over land (1971–96) and ocean (1954–97) from surface observations worldwide*. Oak Ridge, TN: Oak Ridge National Laboratory, Carbon Dioxide Information Analysis Center.

Hartmann, D. L., Ockert-Bell, M. E., & Michelsen, M. L. (1992). The effect of cloud type on Earth's energy balance: Global analysis. *Journal of Climate*, *5*(11), 1281–1304. https://doi.org/10.1175/1520-0442(1992)005<1281:TEOCTO>2.0.CO;2

Henderson, D. S., L'Ecuyer, T., Stephens, G., Partain, P., & Sekiguchi, M. (2013). A multisensor perspective on the radiative impacts of clouds and aerosols. *Journal of Applied Meteorology and Climatology*, *52*(4), 853–871. https://doi.org/10.1175/JAMC-D-12-025.1

Kablick, G. III, Fromm, M., Miller, S., Partain, P., Peterson, D., Lee, S., et al. (2018). The Great Slave Lake PyroCb of 5 August 2014: Observations, simulations, comparisons with regular convection, and impact on UTLS water vapor. *Journal of Geophysical Research: Atmospheres*, *123*, 12,332–312,352. https://doi.org/10.1029/2018JD028965

Kazil, J., Yamaguchi, T., & Feingold, G. (2017). Mesoscale organization, entrainment, and the properties of a closed-cell stratocumulus cloud. *Journal of Advances in Modeling Earth Systems*, *9*, 2214–2229. https://doi.org/10.1002/2017MS001072

King, M. D., Tsay, S.-C., Platnick, S. E., Wang, M., & Liou, K.-N. (1997). Cloud retrieval algorithms for MODIS: Optical thickness, effective particle radius, and thermodynamic phase, MODIS Algorithm Theoretical Basis Document No. ATBD-MOD-05 MOD06 – Cloud product.

L'Ecuyer, T. S., Wood, N. B., Haladay, T., Stephens, G. L., & Stackhouse, P. W. Jr. (2008). Impact of clouds on atmospheric heating based on the R04 CloudSat fluxes and heating rates data set. *Journal of Geophysical Research*, 113, D00A15. https://doi.org/10.1029/2008JD009951

Li, Z., Rosenfeld, D., & Fan, J. (2017). Aerosols and their impact on radiation, clouds, precipitation & severe weather events *rep*., Pacific Northwest National Lab.(PNNL), Richland, WA (United States).

Lilly, D. K. (1968). Models of cloud-topped mixed layers under a strong inversion. *Quarterly Journal of the Royal Meteorological Society*, *94*(401), 292–309. https://doi.org/10.1002/qj.49709440106

Mapes, B. E., & Zuidema, P. (1996). Radiative-dynamical consequences of dry tongues in the tropical troposphere. *Journal of the Atmospheric Sciences*, *53*(4), 620–638. https://doi.org/10.1175/1520-0469(1996)053<0620:RDCODT>2.0.CO;2

McNally, A., Watts, P., Smith, J., Engelen, R., Kelly, G., Thépaut, J., & Matricardi, M. (2006). The assimilation of AIRS radiance data at ECMWF. *Quarterly Journal of the Royal Meteorological Society*, *132*(616), 935–957. https://doi.org/10.1256/qj.04.171

Minnis, P., Garber, D. P., Young, D. F., Arduini, R. F., & Takano, Y. (1998). Parameterizations of reflectance and effective emittance for satellite remote sensing of cloud properties. *Journal of the Atmospheric Sciences*, *55*(22), 3313–3339. https://doi.org/10.1175/1520-0469(1998)055<3313:PORAEE>2.0.CO;2

Minnis, P., Heck, P. W., Young, D. F., Fairall, C., & Snider, J. (1992). Stratocumulus cloud properties derived from simultaneous satellite and island-based instrumentation during FIRE. *Journal of Applied Meteorology*, *31*(4), 317–339. https://doi.org/10.1175/1520-0450(1992)031<0317:SCPDFS>2.0.CO;2

Minnis, P., Kratz, D. P., Coakley, J. A. Jr, King, M. D., Garber, D., Heck, P., et al. (1995). Cloud optical property retrieval (subsystem 4.3), Clouds and the Earth's Radiant Energy System (CERES) algorithm theoretical basis document, Volume III: Cloud Analyses and and Determination of Improved Top of Atmosphere Fluxes (Subsystem 4), NASA RP 1376 Vol. 3, edited by CERES Science Team, December, 1995 (pp. 135-176).

Nicholls, S. (1984). The dynamics of stratocumulus: Aircraft observations and comparisons with a mixed layer model. *Quarterly Journal of the Royal Meteorological Society*, *110*(466), 783–820. https://doi.org/10.1002/qj.49711046603

Nicholls, S., & Leighton, J. (1986). An observational study of the structure of stratiform cloud sheets: Part I. structure. *Quarterly Journal of the Royal Meteorological Society*, *112*(472), 431–460. https://doi.org/10.1002/qj.49711247209

Roach, W., & Slingo, A. (1979). A high resolution infrared radiative transfer scheme to study the interaction of radiation with cloud. *Quarterly Journal of the Royal Meteorological Society*, *105*(445), 603–614. https://doi.org/10.1002/qj.49710544508

Rosenfeld, D. (2014). Climate effects of aerosol-cloud interactions. *Science*, *343*(6169), 379–380.

Rosenfeld, D., Andreae, M. O., Asmi, A., Chin, M., Leeuw, G., Donovan, D. P., et al. (2014). Global observations of aerosol-cloud-precipitation-climate interactions. *Reviews of Geophysics*, *52*, 750–808. https://doi.org/10.1002/2013RG000441

Rosenfeld, D., Zheng, Y., Hashimshoni, E., Pöhlker, M. L., Jefferson, A., Pöhlker, C., et al. (2016). Satellite retrieval of cloud condensation nuclei concentrations by using clouds as CCN chambers. *Proceedings of the National Academy of Sciences of the United States of America*, *113*(21), 5828–5834.

Rosenfeld, D., Zhu, Y., Wang, M., Zheng, Y., Goren, T., & Yu, S. (2019). Aerosol-driven droplet concentrations dominate coverage and water of oceanic low-level clouds. *Science*, *363*(6427), eaav0566. https://doi.org/10.1126/science.aav0566

Siems, S. T., Lenschow, D. H., & Bretherton, C. S. (1993). A numerical study of the interaction between stratocumulus and the air overlying it. *Journal of the Atmospheric Sciences*, *50*(21), 3663–3676. https://doi.org/10.1175/1520-0469(1993)050<3663:ANSOTI>2.0.CO;2

Slingo, A. (1990). Sensitivity of the Earth's radiation budget to changes in low clouds. *Nature*, *343*(6253), 49–51. https://doi.org/10.1038/343049a0

Slingo, A., Brown, R., & Wrench, C. (1982). A field study of nocturnal stratocumulus; III. High resolution radiative and microphysical observations. *Quarterly Journal of the Royal Meteorological Society*, *108*(455), 145–165. https://doi.org/10.1002/qj.49710845509

Stephens, G. (1978). Radiation profiles in extended water clouds. I: Theory. *Journal of the Atmospheric Sciences*, *35*(11), 2111–2122. https://doi.org/10.1175/1520-0469(1978)035<2111:RPIEWC>2.0.CO;2

Stephens, G. L. (2005). Cloud feedbacks in the climate system: A critical review. *Journal of Climate*, *18*(2), 237–273. https://doi.org/10.1175/JCLI-3243.1

Stephens, G. L., & Greenwald, T. J. (1991). The Earth's radiation budget and its relation to atmospheric hydrology: 2. Observations of cloud effects. *Journal of Geophysical Research*, *96*(D8), 15,325–15,340. https://doi.org/10.1029/91JD00972

Stevens, B. (2002). Entrainment in stratocumulus-topped mixed layers. *Quarterly Journal of the Royal Meteorological Society*, *128*(586), 2663–2690. https://doi.org/10.1256/qj.01.202

Stevens, B. (2006). Bulk boundary-layer concepts for simplified models of tropical dynamics. *Theoretical and Computational Fluid Dynamics*, *20*(5–6), 279–304. https://doi.org/10.1007/s00162-006-0032-z

Stevens, B., Brogniez, H., Kiemle, C., Lacour, J.-L., Crevoisier, C., & Kiliani, J. (2017). Structure and dynamical influence of water vapor in the lower tropical troposphere. In *Shallow clouds, water vapor, circulation, and climate sensitivity* (pp. 199–225). Cham: Springer.

Stevens, B., & Feingold, G. (2009). Untangling aerosol effects on clouds and precipitation in a buffered system. *Nature*, *461*(7264), 607–613. https://doi.org/10.1038/nature08281

Sun-Mack, S., Minnis, P., Chen, Y., Kato, S., Yi, Y., Gibson, S. C., et al. (2014). Regional apparent boundary layer lapse rates determined from CALIPSO and MODIS data for cloud-height determination. *Journal of Applied Meteorology and Climatology*, *53*(4), 990–1011. https://doi.org/10.1175/JAMC-D-13-081.1

Susskind, J., Barnet, C., & Blaisdell, J. (1998). Determination of atmospheric and surface parameters from simulated AIRS/AMSU/HSB sounding data: Retrieval and cloud clearing methodology. *Advances in Space Research*, *21*(3), 369–384. https://doi.org/10.1016/S0273-1177(97)00916-2

Susskind, J., Barnet, C. D., & Blaisdell, J. M. (2003). Retrieval of atmospheric and surface parameters from AIRS/AMSU/HSB data in the presence of clouds. *IEEE Transactions on Geoscience and Remote Sensing*, *41*(2), 390–409. https://doi.org/10.1109/TGRS.2002.808236

Tao, W. K., Chen, J. P., Li, Z., Wang, C., & Zhang, C. (2012). Impact of aerosols on convective clouds and precipitation. *Reviews of Geophysics*, *50*, RG2001. https://doi.org/10.1029/2011RG000369

Taylor, J., Edwards, J., Glew, M., Hignett, P., & Slingo, A. (1996). Studies with a flexible new radiation code. II: Comparisons with aircraft short-wave observations. *Quarterly Journal of the Royal Meteorological Society*, *122*(532), 839–861. https://doi.org/10.1002/qj.49712253204

Wood, R. (2005). Drizzle in stratiform boundary layer clouds. Part I: Vertical and horizontal structure. *Journal of the Atmospheric Sciences*, *62*(9), 3011–3033. https://doi.org/10.1175/JAS3529.1

Wood, R. (2012). Stratocumulus clouds. *Monthly Weather Review*, *140*(8), 2373–2423. https://doi.org/10.1175/MWR-D-11-00121.1

Wood, R., & Bretherton, C. S. (2004). Boundary layer depth, entrainment, and decoupling in the cloud-capped subtropical and tropical marine boundary layer. *Journal of Climate*, *17*(18), 3576–3588. https://doi.org/10.1175/1520-0442(2004)017<3576:BLDEAD>2.0.CO;2

Zhang, Y., Stevens, B., & Ghil, M. (2005). On the diurnal cycle and susceptibility to aerosol concentration in a stratocumulus-topped mixed layer. *Quarterly Journal of the Royal Meteorological Society: A Journal of the Atmospheric Sciences, Applied Meteorology and Physical Oceanography*, *131*(608), 1567–1583. https://doi.org/10.1256/qj.04.103

Zheng, Y., Rosenfeld, D., & Li, Z. (2016). Quantifying cloud base updraft speeds of marine stratocumulus from cloud top radiative cooling. *Geophysical Research Letters*, *43*, 11,407–11,413. https://doi.org/10.1002/2016GL071185

Zheng, Y., Rosenfeld, D., & Li, Z. (2018). The relationships between cloud top radiative cooling rates, surface latent heat fluxes, and cloud-base heights in marine stratocumulus. *Journal of Geophysical Research: Atmospheres*, *123*, 11,678–611,690. https://doi.org/10.1029/2018JD028579

Zhou, X., & Bretherton, C. S. (2019). Simulation of mesoscale cellular convection in marine stratocumulus: 2. Nondrizzling conditions. *Journal of Advances in Modeling Earth Systems*, *11*, 3–18. https://doi.org/10.1029/2018MS001448